

# An Allyl Uranium(IV) Sandwich Complex: Are $\phi$ Bonding Interactions Possible?

Ivan A. Popov<sup>+, [a, b]</sup> Brennan S. Billow<sup>+, [c]</sup> Stephanie H. Carpenter,<sup>[c]</sup> Enrique R. Batista,<sup>\*[a]</sup> James M. Boncella,<sup>\*[d]</sup> Aaron M. Tondreau,<sup>\*[c]</sup> and Ping Yang<sup>\*[a]</sup>

**Abstract:** A method to explore head-to-head  $\phi$  back-bonding from uranium f-orbitals into allyl  $\pi^*$  orbitals has been pursued. Anionic allyl groups were coordinated to uranium with tethered anilide ligands, then the products were investigated by using NMR spectroscopy, single-crystal XRD, and theoretical methods. The (allyl)silylanilide ligand, *N*-((dimethyl)prop-2-enylsilyl)-2,6-diisopropylaniline (LH), was used as either the fully protonated, singly deprotonated, or doubly deprotonated form, thereby highlighting the stability and versatility of the silylanilide motif. A free, neutral allyl group was observed in  $U(L_1)_2$  (1), which was synthesized by using the mono-deprotonated ligand  $[K][N$ -((dimethyl)prop-2-

enyl)silyl)-2,6-diisopropylanilide] (L1). The desired homoleptic sandwich complex  $U(L_2)_2$  (2) was prepared from all three ligand precursors, but the most consistent results came from using the dipotassium salt of the doubly deprotonated ligand  $[K]_2[N$ -((dimethyl)propenidesilyl)-2,6-diisopropylanilide] (L2). This allyl-based sandwich complex was studied by using theoretical techniques with supporting experimental spectroscopy to investigate the potential for phi ( $\phi$ ) back-bonding. The bonding between  $U^{IV}$  and the allyl fragments is best described as ligand-to-metal electron donation from a two carbon fragment-localized electron density into empty f-orbitals.

## Introduction

Actinide-ligand (An–L) interactions can be described with an increasing degree of accuracy, thereby providing a new opportunity for a more thorough analysis which can reveal new features of the An–L interactions. For example, in a combined

spectroscopic and theoretical study,<sup>[1]</sup> the reported sandwich complex  $U(C_8H_8)_2$ , was found to contain phi ( $\phi$ ) bonding interactions. Although the 5f- $\phi$  mixing with the ligand orbitals was small, it was still appreciable enough to identify its spectroscopic signature. Such a unique bonding mode is possible due to the U back-donation into the unsaturated hydrocarbon  $\pi^*$  system in a “side-to-head” fashion (Figure 1a).<sup>[1]</sup> A recent theoretical study of the experimentally synthesized Cp-supported (Cp = cyclopentadienyl, and its derivatives)  $U^{IV}$  metallacyclocumulene complexes,  $U(\eta^5-C_5Me_5)_2(\eta^4-C_4R_2)$  (R = trimethylsilyl, phenyl), has demonstrated a possibility of another rare type of  $\phi$  interaction, that is, “side-to-side”  $\phi$  U–L back-donation into the cumulene  $\pi^*$  system (Figure 1b).<sup>[2]</sup> In contrast to  $U(C_8H_8)_2$ , it was found that the  $\phi$  bonding in the series of An metallacyclocumulenes, especially in the cases of U and Pa, is much more pronounced. In fact, it is comparable to the L–An  $\pi$  bonding interactions, which, altogether with L–An  $\sigma$  interactions ( $\sigma + \pi + \phi$ ), help to counter the impact of the An contraction in the series from Th to Pu.<sup>[2]</sup>

Allyl anion ligands are not routinely considered ligands for the generation of organometallic sandwich complexes, nor are they cumulenes, but the coordination modes of uranium f-orbitals with the allyl  $\pi$ -system relate to both previously described systems. With two orbitals filled that can donate to the metal – the fully bonding and nonbonding combinations – one fully antibonding  $\pi^*$  orbital remains that is able to accept bonding electron density from the uranium center (Figure 1c). In the case of two allyl ligands coordinating to U, six lobes that comprise the  $\pi^*$  orbitals of the diallyl system may be available for the  $\phi$  back-donation in a “head-to-head” fashion (Figure 1d), which is the last missing link out of all possible An–L  $\phi$ -back-bonding modes. Alternatively, the filled allyl  $\pi$ -system can act

[a] I. A. Popov,<sup>+</sup> E. R. Batista, P. Yang  
Theoretical Division, Los Alamos National Laboratory  
Los Alamos, New Mexico 87545 (USA)  
E-mail: erb@lanl.gov  
pyang@lanl.gov

[b] I. A. Popov<sup>+</sup>  
Current address: Department of Chemistry  
The University of Akron  
Akron, Ohio 44325-3601 (USA)

[c] B. S. Billow,<sup>+</sup> S. H. Carpenter, A. M. Tondreau  
Chemistry Division  
Los Alamos National Laboratory  
MS J514, Los Alamos, New Mexico 87545 (USA)  
E-mail: tondreau\_a@lanl.gov

[d] J. M. Boncella  
Department of Chemistry, Washington State University  
and Pacific Northwest National Laboratory  
Pullman, Washington 99164  
and  
902 Batelle Blvd, Richland, Washington 99352 (USA)  
E-mail: james.boncella@wsu.edu

[<sup>+</sup>] These authors contributed equally to this work.

Supporting information for this article is available on the WWW under <https://doi.org/10.1002/chem.202200114>

© 2022 The Authors. Chemistry - A European Journal published by Wiley-VCH GmbH. This is an open access article under the terms of the Creative Commons Attribution Non-Commercial NoDerivs License, which permits use and distribution in any medium, provided the original work is properly cited, the use is non-commercial and no modifications or adaptations are made.

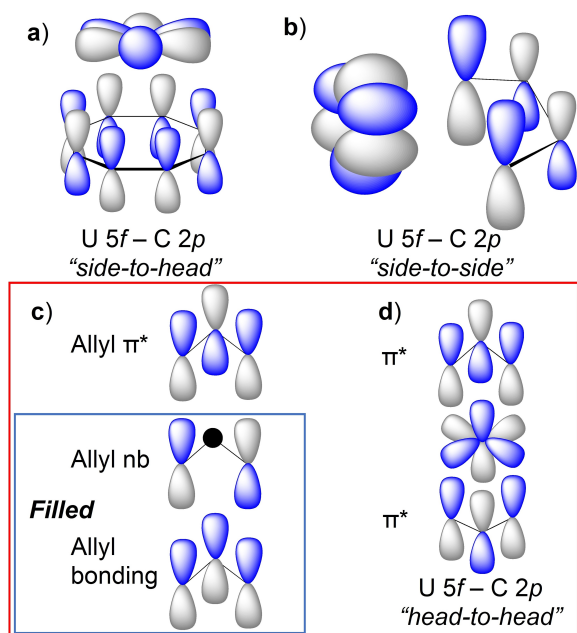


**Figure 1.** Representations of a) "side-to-head" and b) "side-to-side"  $\phi$  interactions. c) The  $\pi$ -system of allyl anion, and d) the resulting desired "head-to-head"  $\phi$ -bonding interaction between a uranium f-orbital and the  $\pi^*$  diallyl orbitals.

as an electron donor into empty f-orbitals of the metal. Natural questions that arise are fundamentally important in actinide coordination: are the filled molecular orbitals of a  $U^{IV}$  center high enough in energy to donate electron density into allyl  $\pi^*$  orbitals? Or will the interaction occur exclusively due to the donation of electron density from the filled allyl  $\pi$ -bonding orbitals into the empty U f-orbitals?

Uranium allyl bonds remain a rare coordination event even as the number of uranium carbon bonds continues to expand,<sup>[3]</sup> whereas lanthanide-allyl bonds have been much more thoroughly investigated.<sup>[4]</sup> Cp-supported uranium allyl complexes have been studied, with reports on the allyl ligands coordinating in both  $\eta^1$  and  $\eta^3$  modes in these systems.<sup>[5]</sup> Outside of Cp-supported examples, there are only a handful of uranium-allyl interactions described in the literature. Early examples of uranium allyl bonding include the extremely sensitive homoleptic compounds,  $U(\text{allyl})_4$  and  $U(\text{allyl})_3$ , both of which degrade thermally above  $-20^\circ\text{C}$ .<sup>[6]</sup> Analogous complexes can be found in the  $U(\text{allyl})_3(\text{X})$  series ( $\text{X}=\text{Cl}, \text{Br}, \text{or I}$ ),<sup>[7]</sup> which are highly sensitive to thermal degradation. Hanusa's work with allyl thorium complexes showed that the use of bulky allyl ligands generates thermally stable species.<sup>[8]</sup> The homoleptic allyl complexes have been used in alcoholysis reactions to give well-defined uranium-allyl derivatives.<sup>[9]</sup> Unfortunately, there has been little in the way of theoretical studies of the bonding interactions between the f-orbitals and the allyl  $\pi$ -system.

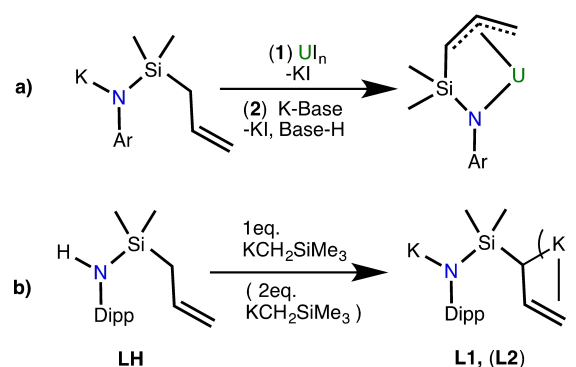
Organometallic sandwich complexes of uranium have been known since 1956, with early examples of cyclopentadiene (Cp),<sup>[10]</sup> followed by cyclooctatetraene (COT),<sup>[11]</sup> complexes representing the birth of organometallic uranium chemistry.

Further work explored the reactivity of the mixed COT, Cp sandwich complexes.<sup>[12]</sup> These  $\eta^8$  and  $\eta^5$  bonded complexes are the basis of further exploration into  $\pi$ -bonded aromatic uranium sandwich complexes. Uranium-arene  $\eta^6$  interactions have been known for five decades and have been shown to be robust,<sup>[13]</sup> likely due to  $\delta$ -bonding,<sup>[14]</sup> although few examples of bis- $\eta^6$  sandwich complexes are known.<sup>[15]</sup> Additionally, there are reports of sandwich complexes synthesized using cycloheptatrienyl<sup>[16]</sup> and cyclobutadienyl<sup>[17]</sup> ligands. The field continues to grow and generate interest, specifically in the bonding between the f-orbitals and the unsaturated organic  $\pi$ -orbitals. This work employs allyl-anion ligands to expand the known sandwich complexes of uranium.

Tethering allyl groups to a Cp ligand has provided successful coordination of neutral propenyl moieties to lanthanide complexes.<sup>[18]</sup> Silylated Tren (Tren = tris(2-aminoethyl)amine) ligand scaffolds have been shown to impart stability towards uranium complexes.<sup>[19]</sup> Previously, (silyl)amide ligands were used to generate robust, crystalline uranium complexes bearing four (trimethylsilyl)(alkyl)amide ligands to study iso-structural  $U^{IV/V}$  compounds.<sup>[20]</sup> By tethering an allyl(dimethyl)silyl group to an aniline, the stability of U-silylamides would be retained while creating proximity between the metal center and the allyl fragment to encourage bonding (Scheme 1a). A new organometallic sandwich complex comprising six carbon atoms of two allyl ligands coordinating uranium was targeted, where the synthesis and use of three ligand derivatives (fully protonated, singly deprotonated, and doubly deprotonated; Scheme 1b) and their reactivity with uranium are explored. The detailed chemical bonding analysis of the U–L interactions is given, thus answering the questions about their bonding nature, and, specifically, addressing the possibility of the anticipated  $\phi$  back-donation.

## Results and Discussion

*N*-((Dimethyl)prop-2-enylsilyl)2,6-diisopropylaniline, LH, was synthesized by the addition of allylchloro(dimethyl)silane to Li-



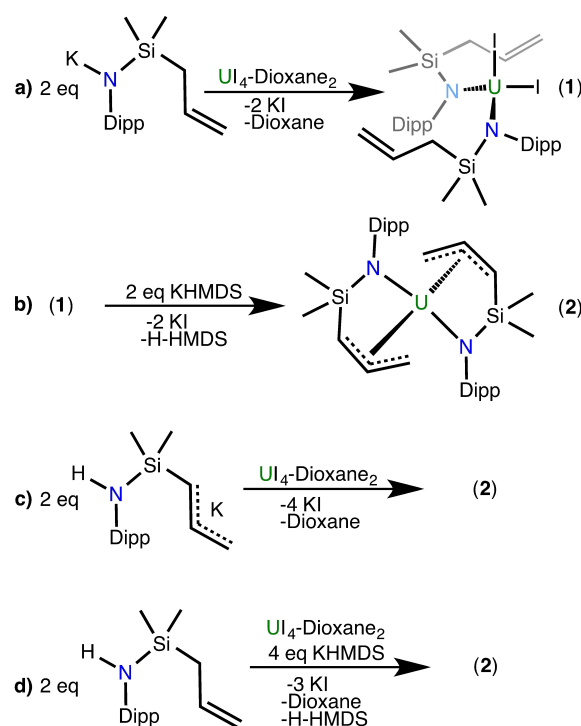
**Scheme 1.** a) Generalized synthetic scheme to achieve allyl coordination to uranium through an anilide tether; (Ar = aryl group). b) The three hypothesized protonation states of our investigated ligand motif, from the fully protonated LH to the singly and doubly deprotonated ligands L1 and L2; (Dipp = 2,6-diisopropylphenyl).

NHDipp.<sup>[21]</sup> The mono-deprotonation of LH was achieved by addition of a single equivalent of (trimethylsilyl)methylpotassium (KNSi) to LH in *n*-hexane to generate [K][N-((dimethyl)prop-2-enyl)silyl]-2,6-diisopropylanilide (L1, Scheme 1b), which was isolated as the base-free salt as observed by single-crystal X-ray diffraction (SC-XRD; Figure S12 in the Supporting Information). The <sup>1</sup>H NMR and <sup>13</sup>C NMR spectra were consistent with the single deprotonation of the N–H portion of the ligand; the N–H resonance of LH (2.14 ppm) is absent in the spectrum of L1, but the CH<sub>2</sub> protons of the allyl moiety are present in both spectra as doublets at 1.62 ppm for LH and 1.58 ppm for L1. The <sup>13</sup>C {<sup>1</sup>H} NMR spectrum also contained resonances consistent with a neutral propene.

LH was doubly deprotonated by the addition of two equivalents of KNSi in diethyl ether to yield the corresponding dianionic compound [K]<sub>2</sub>[N-((dimethyl)propenidesilyl)-2,6-diisopropylanilide] (L2, Scheme 1b) as a yellow crystalline material. The <sup>1</sup>H NMR spectrum collected in [D<sub>8</sub>]THF revealed two conformational isomers of the product in solution (Figure S10a, b). SC-XRD studies of L2 crystallized from the reaction solution of diethyl ether show L2 as a two-dimensional, linear polymer in the solid-state with a single solvent molecule (Figure S13). Crystallization of L2 from [D<sub>8</sub>]THF reveals a solid-state structure with a different geometric conformation, and the molecule is folded in rather than linear (the allyl is *syn* to the arene, rather than *anti*, due to rotation around the Si–N bond). Both potassium atoms are bound η<sup>3</sup> to the allyl anion, with one of the potassium atoms bound η<sup>6</sup> to the arene ring, and the other coordinated to THF (Figure S14).

The reaction of these ligands with U<sub>4</sub>(1,4-dioxane)<sub>2</sub> was performed in toluene to limit the coordination of undesired Lewis-base solvent molecules to the metal center.<sup>[22]</sup> The addition of two equivalents of L1 to U<sub>4</sub>(1,4-dioxane)<sub>2</sub> resulted in the dissolution of the chalky red slurry of the starting uranium material to give a brown/red solution over the course of 10 minutes at room temperature. The brown/red powder of U<sub>2</sub>(L1)<sub>2</sub> (1, Scheme 2a) was isolated in moderate yield. The <sup>1</sup>H NMR spectrum of 1 contained seven broad resonances that integrate roughly to the expected ratios for the freely rotating ligand of a C<sub>2v</sub> symmetric complex. An Evans measurement of 1 was obtained in C<sub>6</sub>D<sub>6</sub>, giving a room-temperature magnetic moment of 2.2 μ<sub>B</sub>.

SC-XRD experiments performed on 1 yielded the monoclinic space group P2<sub>1</sub>/n with a single molecule in the asymmetric unit (Figure 2). The uranium center was found in a pseudo-tetrahedral environment with angles of 116.67(11)° for the N–U–N bond and 108.55(13)° for the I–U–I bond. The *ipso*-carbon atoms of the aryl groups appeared to be interacting with the uranium center, and this secondary interaction likely gives rise to the averaged short U–amide bonds of 2.180(5) Å, a feature noted previously in aryl amide compounds.<sup>[23]</sup> The propenyl fragments of 1 were not coordinated to the U-center, and the carbon alpha (C(13)) to the silicon of the propenyl fragment remains tetrahedral, indicating a neutral propenyl group. The C–C bond distances of the allyl moiety of 1 are consistent with those of L1, with C(13)–C(14) found to be 1.504(5) Å in 1 and 1.488(16) Å in L1 and the terminal carbon



**Scheme 2.** Synthetic scheme outlining the synthesis of uranium complexes 1 and 2.

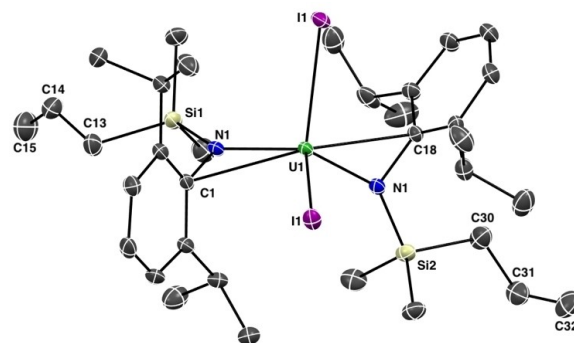


**Figure 2.** The solid-state structure of 1 is presented with ellipsoids at 50% probability and hydrogen atoms removed for clarity.

bonds, C(14)–C(15), found at 1.307(6) Å for 1 and 1.324(2) Å in L1.

Upon dehydrohalogenation of 1 with potassium bis(trimethylsilyl)amide (KHMDS) in a toluene solution, the red coloration of the solution deepened and the appearance of KI precipitate was observed. Filtration of the salt and removal of toluene led to a tacky dark red solid, which was triturated with pentane; the pentane phase was cooled and X-ray quality crystals formed. Volatiles were removed from the remaining red material, leaving brick-red powder that was assigned as U(L2)<sub>2</sub> (2, Scheme 2b). Complex 2 was also synthesized by adding solid L2 to a cold toluene slurry of U<sub>4</sub>(1,4-dioxane)<sub>2</sub>. Analysis of the isolated red product confirmed the generation of 2 from this method (Scheme 2c). One additional synthetic method to

generate **2** was performed by mixing two equivalents of LH with  $U_4(1,4\text{-dioxane})_2$ , followed by addition of four equivalents of KHMDS to the cold reaction slurry. Analysis of the isolated material confirmed the formation of **2** (Scheme 2d), albeit in lower isolated yields than the other two methods. **2** was observed to be persistent under inert conditions at room temperature for extended periods of time.

The  $^1\text{H}$  NMR spectrum of **2** contained 15 resonances, consistent with the expected number of resonances for a static structure (Figure S11). All allyl-proton resonances were observed, where prior examples of  $U^{IV}$  allyl fragments had the terminal allylic C–H resonance absent in the  $^1\text{H}$  NMR spectrum.<sup>[5d,e]</sup> An Evans measurement was obtained in  $C_6D_6$ , revealing a room-temperature magnetic moment of  $2.5 \mu_B$ , which, much like **1**, is low for two unpaired electrons, but consistent with the spin-orbit coupling observed for uranium systems.<sup>[24]</sup> SC-XRD experiments performed showed that **2** crystallized in the orthorhombic space group  $Fdd2$ , wherein the asymmetric unit is composed of half of the molecule. The propenyl fragments of **2** were coordinated to the uranium center, bound  $\eta\text{-}3$  (Figure 3) in a sandwich-like coordination environment. The *ipso*-carbon atoms of the aryl groups were no longer directed towards the metal and appear non-interacting, and the U–amide bonds lengthened to 2.210(2) Å. The carbon alpha (C(13)) to the silicon of the propenyl fragment was deprotonated, confirming the formation of anionic propenyl groups. The C–C bond distances of the allyl moiety of **2** are clearly distinct from those of **1**, with a shortened C(13)–C(14) bond at 1.403(4) Å and an elongated C(14)–C(15) bond at 1.385(4) Å.

A theoretical investigation was conducted on **2** to determine the nature of the U–allyl interactions. The calculated structural metrics of the computed complex **2** ( $C_2$ , triplet spin state) are in excellent agreement with the SC-XRD data (Table S1), with the bond distances and angles within 1.5 and 2% of the experiment, respectively, providing confidence in the theoretical model (see the Supporting Information for computational methodology and details of the calculations). Positioning of the C atoms of the allyl ligands with respect to the U center in **2** is similar to that of the previously reported U metallacyclocumulene complex  $U(\eta^5\text{-C}_5\text{Me}_5)_2(\eta^4\text{-C}_4\text{R}_2)$  (R = trimeth-

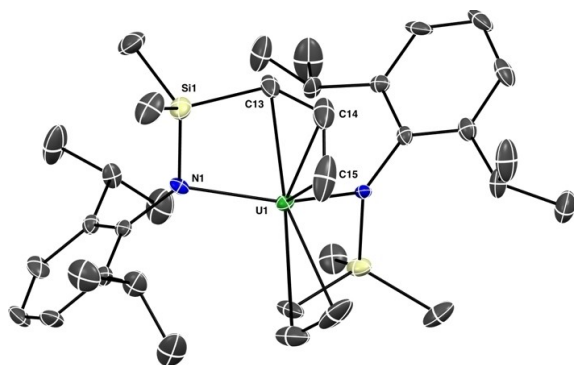


**Figure 3.** The grown solid-state structure of **2** is presented with ellipsoids at 50% probability and hydrogen atoms removed for clarity.

ylsilyl, phenyl)<sup>[2c]</sup> exhibiting the so-called “in-plane” An–L interaction.<sup>[2a]</sup> Specifically, U is just 0.005 Å away from the cumulene plane in the U metallacyclocumulenes while it resides exactly in the diallyl plane in **2**, that is, 0.000 Å to the plane. As found previously in the  $An^{IV}$  metallacycles,<sup>[2a]</sup> the “in-plane” positioning of the An and L atoms may play an important role in enhancing the covalent An–L  $\sigma$ ,  $\pi$ ,  $\delta$ , and  $\phi$  interactions that could even defy the commonly accepted  $An^{IV}$  contraction trend in the Pa–Pu series. Hence, it is also anticipated to see enhanced covalent interactions in **2** due to covalent overlap between the 5f orbitals of U and 2p C orbitals of the two anionic allyl groups.

To understand the nature of the U–diallyl bonding from the electronic structure perspective, a chemical bonding analysis was performed. Because of the complexity of the canonical molecular orbitals (CMOs, Figure S1), which are intrinsically difficult to interpret in terms of chemical bonds due to delocalization, natural bond orbital (NBO)<sup>[25]</sup> and adaptive natural density partitioning (AdNDP)<sup>[26]</sup> analyses were performed using AdNDP 2.0 code,<sup>[27]</sup> thus enabling the search for both localized (one-center (1c) and two-center (2c)) and multi-center ( $nc$ ,  $n > 2$ ) bonding interactions. Like  $An^{IV}$  metallacyclocumulenes where An–L  $\phi$  interactions occur due to the promotion of some electron density from the frontier orbitals of the metal to the antibonding orbitals of the ligand,<sup>[2a]</sup> the two top molecular orbitals (MOs) in **2** (Figures S1b and S2) are also 5f-dominant (81.1% U 5f in HOMO, 76.4% U 5f in HOMO-1), and can potentially contribute to the An–L interactions through back-donation.

However, according to AdNDP, these two CMOs are transformed into two very localized one-center, one-electron (1c–1e) elements on U (i.e., two unpaired U 5f electrons, Figure 4a) exhibiting 99.6–99.7% f-character, with high occupation numbers (ON = 0.98–0.99 |e|), and, hence, no appreciable An–L back-donation is found. The major bonding interaction between the U ion and two allyl moieties occurs due to the formation of four three-center two-electron (3c–2e) U–C–C  $\sigma$  bonds (Figure 4b) originating from the four delocalized CMOs, that is, HOMO-2, HOMO-3, HOMO-12, and HOMO-24 (Figure S1c), which are responsible for the U–diallyl  $\sigma$  interactions. These bonds are highly polarized towards C atoms (~85.9% of the electron density per bond, Table S2), and are formed due to the interaction of the 2s2p hybrid orbitals of the three C atoms ( $C_{\text{term}}$  (C15),  $C_{\text{centr}}$  (C14), and  $C_{\text{alpha}}$  (C13)) with the hybrid orbitals of U composed of primarily 6d5f characters (~79.0–87.4%; Table S3).

Principally, two 3c–2e  $\sigma$  bonds of each allyl fragment can be seen as a product of interaction of the two  $\pi$  bonds ( $C_{\text{alpha}}\text{--}C_{\text{centr}}$  and  $C_{\text{term}}\text{--}C_{\text{centr}}$ ) of the silylallyl anion (Figure S3) aligned head-on with the U orbitals in **2**. These two C–C  $\pi$  bonds of the silylallyl anion ligand arise from the two frontier  $\pi$  CMOs, that is, HOMO and HOMO-1 (Figure S3), which look very similar to the four aforementioned CMOs of **2** at each allyl ligand. The  $C_{\text{alpha}}\text{--}C_{\text{centr}}$   $\pi$  bond in the silylallyl anion has somewhat lower ON value (1.73 |e|), in accordance with its longer bond length of 1.417 Å as compared to the adjacent  $C_{\text{term}}\text{--}C_{\text{centr}}$   $\pi$  bond with ON = 1.99 |e| (Figure S3) corresponding to the shorter bond

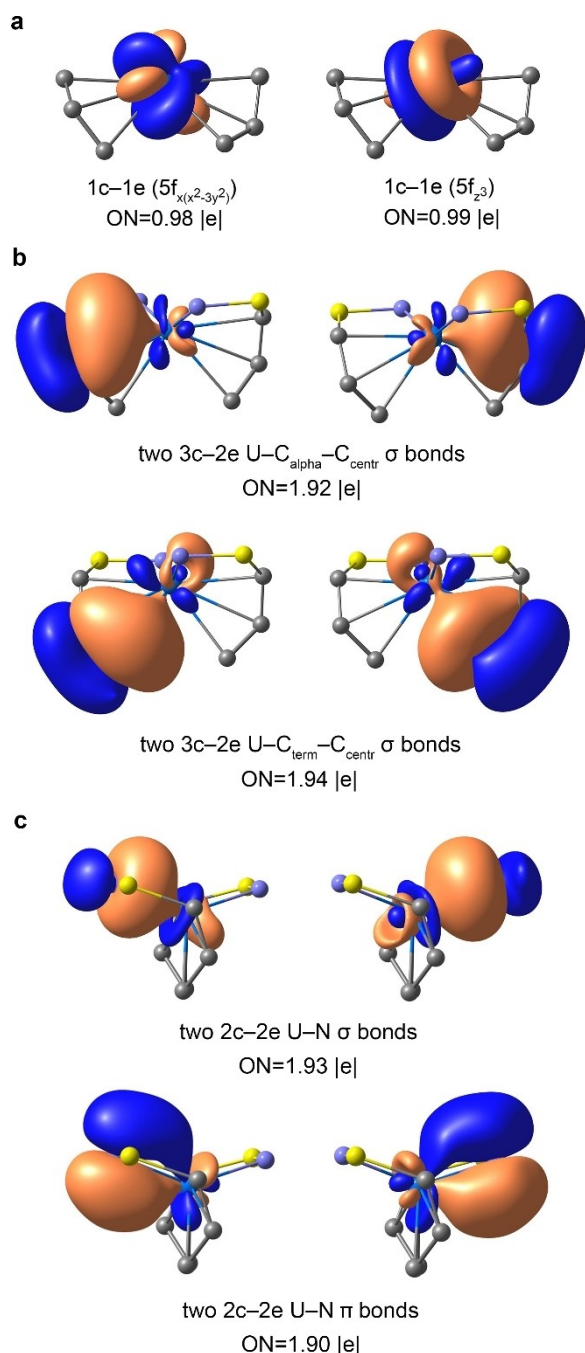


**Figure 4.** U, U-C, U-N AdNDP elements found in **2**. a) Two unpaired 5f-electrons on U. b) Four 3c-2e U-C  $\sigma$  bonds. c) Four 2c-2e U-N bonds. ON denotes occupation number. ON is equal to 2.00 |e| or 1.00 |e| in an ideal case for a doubly or singly occupied bond, respectively. U is blue, C is gray, N is light violet, and Si is yellow.

length of 1.367 Å. However, upon interaction with the U center, the C<sub>alpha</sub>-C<sub>centr</sub> and C<sub>term</sub>-C<sub>centr</sub> bonds become almost equal in **2**, that is, 1.403 Å and 1.392 Å, respectively, in accordance with the similar ON values of the corresponding U-C<sub>alpha</sub>-C<sub>centr</sub> (ON = 1.92 |e|) and U-C<sub>term</sub>-C<sub>centr</sub> (ON = 1.94 |e|)  $\sigma$  bonds and similar U contributions in these bonds, both of ~14.1% (Table S2).

The 3c-2e delocalized bonding is principally considered a weaker interaction compared to the direct 2c-2e U-C bonding (given the same ON values and bond polarization), giving rise to longer bond lengths; the average U-C bond length in **2** (2.645 Å) is appreciably larger than the sum of the covalent radii for a single U-C bond (2.450 Å).<sup>[28]</sup> Indeed, the four 3c-2e  $\sigma$  bonds with ON = 1.92–1.94 |e| can be represented as four direct 2c-2e U-C  $\sigma$  bonds: two U-C<sub>term</sub> and two U-C<sub>alpha</sub>  $\sigma$  bonds (Figure S4a), but with significantly lower ON values (1.53–1.57 |e|), and hence were not accepted in the AdNDP search. This shows that the C<sub>centr</sub> atom is the minor contributor to the 3c-2e  $\sigma$  bonds. Specifically, the C<sub>term</sub>/C<sub>alpha</sub> atoms of the allyl fragments account for ~64.7–67.5% of the electron density per 3c-2e bond, and only ~18.4–21.1% comes from C<sub>centr</sub> (Table S2). This explains the appreciably shorter U-C<sub>term</sub> (2.619 Å) and U-C<sub>alpha</sub> (2.603 Å) bond distances as compared to U-C<sub>centr</sub> (2.714 Å; Table S1). This is also in accordance with the C atom contributions in the  $\pi$  bonding of the parental silylallyl anion considered alone, wherein the C<sub>term</sub> (67.8%) and C<sub>alpha</sub> (87.3%) atoms are also the major providers of the 2p electron density available for the interaction with the metal. Alternatively, two 3c-2e  $\sigma$  bonds found over each allyl ligand in **2** can also be viewed as two 4c-2e U-C<sub>term</sub>-C<sub>centr</sub>-C<sub>alpha</sub>  $\sigma$  bonds (Figure S4c), which are reminiscent of the CMOs responsible for the U-diallyl  $\sigma$  interactions discussed earlier (Figure S1c). However, their ON values are larger by only 0.03 |e| on average, and, hence, the 3c-2e bonding picture with the smaller number of centers was accepted instead, per the AdNDP procedure.<sup>[26]</sup>

To summarize, the organometallic framework described here is geometrically appropriate for the observation of head-to-head  $\phi$ -bonding between the f-orbitals of the uranium center and the allyl  $\pi^*$  fragments, but the energetics of the corresponding orbitals are not. In order to attain electron donation from the metal to the  $\pi^*$  orbitals of the allyl groups, the energy of the f-orbitals will need to be higher. Moving forward, this will be achieved in one of two ways: using a more reduced uranium center, or by adapting the chemistry to transuranic elements Np and Pu. The increased electron density at the metal, in the same geometric configuration, may generate the desired M-to-L  $\phi$ -bonding.

The U-N interactions in **2** can be described as direct 2c-2e  $\sigma$  bonds with some contribution from the N 2p orbitals promoting the electron density into the U 6d5f hybrids by forming  $\pi$  bonding interactions (Figure 4c). Both U-N  $\sigma$  and  $\pi$  bonds, which originate from the four CMOs, that is, HOMO-4, HOMO-5, HOMO-8, and HOMO-9 (Figure S1d), are even more ionic than the U-C-C bonding, with ~87.0–87.4% of the electron density coming from the N atoms per bond (Table S2). Overall, based on their bond distances (2.236 Å theor. vs. 2.210 Å exp.) and the bonding analysis, the U-N bonds can be regarded as intermediate between single and double bonds, in accordance with the sum of their covalent bond radii,<sup>[28]</sup> that is, 2.410 and 1.940 Å for single and double U-N bonds, respectively.

The UV/Vis spectrum obtained of **2** in toluene (1.0 mmol in solution) shows a broad, rapid increase in absorbance beginning at ~580 nm, with very few distinct features as the

spectrum approaches 350 nm. The computed spectrum qualitatively follows the experimental spectrum in shape, with increasing absorbance between 500 and 350 nm, but is far more detailed than what was obtained experimentally (Figure S7).

According to the natural transition orbital (NTO) analysis<sup>[29]</sup> of **2**, the energy region in ~350–500 nm range is dominated by the f–d transitions exhibiting low oscillator strength values (Figure S6). These transitions originate from the top two 5f-dominant HOMOs to the lowest unoccupied MOs (LUMOs) with dominant d-character, that is, LUMO+5, LUMO+6 (Figure S1a). In the higher energy region at ~220–350 nm, complex **2** exhibits primarily ligand-to-metal charge transfer (LMCT) excitations originating from either 2p C orbitals of allyls or benzene fragments or 2p N orbitals to 6d or 5f orbitals of U (Figure 5). Higher-energy ligand-to-ligand charge transfer (LLCT) excitations involving various 2p C and 2p N ligand orbitals start appearing at ~220 nm.

## Conclusion

Complex **2** represents a theory-driven synthetic effort aimed explicitly to address a shortfall in fundamental data in f-orbital covalency with unsaturated carbon fragments. By taking advantage of a close collaboration between theoretical and synthetic scientists, a description of a missing link – head-to-head  $\phi$ -bonding interactions in uranium f-orbitals – was pursued. Using a tethering method to bring an allyl moiety within bonding distance of a uranium center using a silyl-anilido ligand, a new diallyl sandwich complex of uranium was prepared and studied. The judicious choice of ligand motif led to the isolation of unbound, neutral allyl fragments of **1**, which served as both a precursor and a control complex, in which the metrical parameters could be used as a point of comparison. The isolated diallyl-sandwich complex **2** was synthesized with three different methods by using the tunable protonation states of LH, L1, and L2. The variety and general success of our methodologies confirms our rationale for the use of this ligand

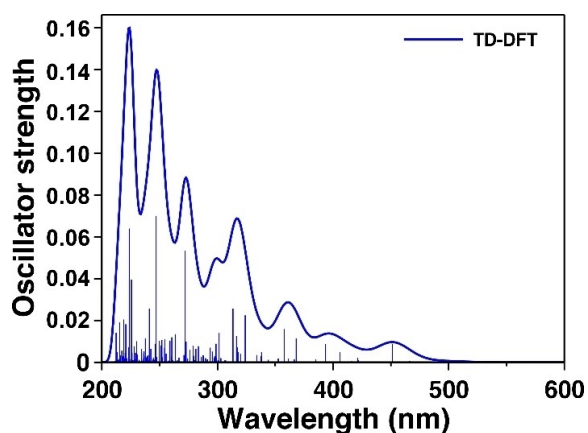


Figure 5. Computed TD-DFT spectrum of **2**. Vertical bars depict the theoretical oscillator strength of single-electron excitations.

motif and the stabilization of organometallic sandwich complexes.

Computational assessment of **2** revealed a much more nuanced bonding scheme between uranium and the allyl fragments than the desired  $\phi$ -bonding. There appears to be no  $\phi$ -bonding into the  $\pi^*$  system of the allyl fragments of the complex, rather the filled allyl  $\pi$ -bonding orbitals donate electron density into the uranium-based orbitals. Additionally, this donation occurs in a very localized manner between two contiguous carbon atoms of the allyl fragment and the uranium center, thereby generating a three-center, two-electron bonding interaction. Due to the perfect in-plane positioning of the U and C atoms of the diallyl, the U–C interactions show strong covalent character with a significant U contribution of ~14.1%. The better energy match is observed between the filled  $\pi$ -bonding orbitals and the empty uranium f-orbitals, rather than the desired match between the  $\pi^*$  orbitals and the filled uranium f-orbitals. We will continue to pursue this investigation into the as-of-yet unknown head-to-head  $\phi$ -bonding.

## Supporting information

Deposition Numbers 2095679 (for L1), 2095680 (for L2), 2095681 (for L2b), 2095682 (for 1), 2095683 (for 2) contain the supplementary crystallographic data for this paper. These data are provided free of charge by the joint Cambridge Crystallographic Data Centre and Fachinformationszentrum Karlsruhe Access Structures service.

## Acknowledgements

This work was conceived and executed at Los Alamos National Laboratory. This work was supported by the US Department of Energy through the Los Alamos National Laboratory. Los Alamos National Laboratory is operated by Triad National Security, LLC, for the National Nuclear Security Administration of U.S. Department of Energy (Contract no. 89233218CNA000001). This work was mainly sponsored by the US Department of Energy, Chemical Sciences, Geosciences, and Biosciences Division, Heavy Element Chemistry program, under contract DE-AC52-06NA25396. I.A.P. acknowledges support from a J. Robert Oppenheimer Distinguished Postdoctoral Fellowship at Los Alamos National Laboratory. A.M.T. and S.H.C. acknowledge Seaborg Institute-funded post-doctoral fellowships from Los Alamos National Laboratory for support in addition to funding from the Heavy Element Chemistry program.

## Conflict of Interest

The authors declare no conflict of interest.

## Data Availability Statement

The data that support the findings of this study are available in the supplementary material of this article.

**Keywords:** allyl · anilides · organometallic · phi-bonding · uranium

- [1] S. G. Minasian, J. M. Keith, E. R. Batista, K. S. Boland, D. L. Clark, S. A. Kozimor, R. L. Martin, D. K. Shuh, T. Tyliczszak, *Chem. Sci.* **2014**, *5*, 351–359.
- [2] a) M. P. Kelley, I. A. Popov, J. Jung, E. R. Batista, P. Yang, *Nat. Commun.* **2020**, *11*, 1558; b) J. K. Pagano, J. Xie, K. A. Erickson, S. K. Cope, B. L. Scott, R. Wu, R. Waterman, D. E. Morris, P. Yang, L. Gagliardi, J. L. Kiplinger, *Nature* **2020**, *578*, 563–567; c) J. K. Pagano, K. A. Erickson, B. L. Scott, D. E. Morris, R. Waterman, J. L. Kiplinger, *J. Organomet. Chem.* **2017**, *829*, 79–84.
- [3] a) S. A. Johnson, S. C. Bart, *Dalton Trans.* **2015**, *44*, 7710–7726; b) S. T. Löffler, K. Meyer, in: *Comprehensive Coordination Chemistry III* (Eds.: E. C. Constable, G. Parkin, L. Que, Jr), Elsevier, Oxford, **2021**, pp. 471–521; c) D. R. Hartline, K. Meyer, *JACS* **2021**, *1*, 698–709; d) C. E. Hayes, D. B. Leznoff, *Coord. Chem. Rev.* **2014**, *266–267*, 155–170; e) F. T. Edelmann, J. H. Farnaby, F. Jaroschik, B. Wilson, *Coord. Chem. Rev.* **2019**, *398*, 113005; f) J. H. Farnaby, T. Chowdhury, S. J. Horsewill, B. Wilson, F. Jaroschik, *Coord. Chem. Rev.* **2021**, *437*, 213830; g) J. Murillo, S. Fortier, *Actinides: Pentavalent Organometallics*, in *Encyclopedia of Inorganic and Bioinorganic Chemistry*, eds. W. J. Evans and T. P. Hanusa, Wiley, **2018**, p. eibc2544; h) S. Fortier, B. C. Melot, G. Wu, T. W. Hayton, *J. Am. Chem. Soc.* **2009**, *131*, 15512–15521.
- [4] a) J.-F. Carpentier, S. M. Guillaume, E. Kirillov, Y. Sarazin, *C. R. Chim.* **2010**, *13*, 608–625; b) E. J. Waheed, A. A. R. Ahmed, A. T. Numan, *Ann. Romanian Soc. Cell Biol.* **2021**, *25*, 228–245; c) R. D. Dicken, A. Motta, T. J. Marks, *ACS Catal.* **2021**, *11*, 2715–2734; d) F. T. Edelmann, D. M. M. Freckmann, H. Schumann, *Chem. Rev.* **2002**, *102*, 1851–1896; e) F. T. Edelmann, *Angew. Chem. Int. Ed. Engl.* **1995**, *34*, 2466–2488; *Angew. Chem.* **1995**, *107*, 2647–2669; f) J. Jothieswaran, S. Fadlallah, F. Bonnet, M. Visseaux, *Catalysts* **2017**, *7*, 378/371–378/314.
- [5] a) C. L. Webster, J. W. Ziller, W. J. Evans, *Organometallics* **2013**, *32*, 4820–4827; b) G. W. Halstead, E. C. Baker, K. N. Raymond, *J. Am. Chem. Soc.* **1975**, *97*, 3049–3052; c) T. J. Marks, A. M. Seyam, J. R. Kolb, *J. Am. Chem. Soc.* **1973**, *95*, 5529–5539; d) T. H. Cymbaluk, R. D. Ernst, V. W. Day, *Organometallics* **1983**, *2*, 963–969; e) C. L. Webster, J. W. Ziller, W. J. Evans, *Organometallics* **2012**, *31*, 7191–7197.
- [6] G. Lugli, W. Marconi, A. Mazzei, N. Palladino, U. Pedretti, *Inorg. Chim. Acta* **1969**, *3*, 253–254.
- [7] G. Lugli, A. Mazzei, S. Poggio, *Makromol. Chem.* **1974**, *175*, 2021–2027.
- [8] C. N. Carlson, T. P. Hanusa, W. W. Brennessel, *J. Am. Chem. Soc.* **2004**, *126*, 10550–10551.
- [9] M. Brunelli, G. Perego, G. Lugli, A. Mazzei, *J. Chem. Soc. Dalton Trans.* **1979**, *5*, 861–868.
- [10] a) L. T. Reynolds, G. Wilkinson, *J. Inorg. Nucl. Chem.* **1956**, *2*, 246–253; b) F.-S. Guo, Y.-C. Chen, M.-L. Tong, A. Mansikkamaeki, R. A. Layfield, *Angew. Chem. Int. Ed.* **2019**, *58*, 10163–10167; *Angew. Chem.* **2019**, *131*, 10269–10273; c) F.-S. Guo, N. Tsoureas, G.-Z. Huang, M.-L. Tong, A. Mansikkamaeki, R. A. Layfield, *Angew. Chem. Int. Ed.* **2020**, *59*, 2299–2303; *Angew. Chem.* **2020**, *132*, 2319–2323.
- [11] a) A. Streitwieser Jr., U. Mueller-Westerhoff, *J. Am. Chem. Soc.* **1968**, *90*, 7364; b) J. T. Boronski, A. J. Wooles, S. T. Liddle, *Chem. Sci.* **2020**, *11*, 6789–6794; c) F. M. Sroor, *J. Organomet. Chem.* **2021**, *948*, 121878.
- [12] a) A. R. Schake, L. R. Avens, C. J. Burns, D. L. Clark, A. P. Sattelberger, W. H. Smith, *Organometallics* **1993**, *12*, 1497–1498; b) W. J. Evans, G. W. Nyce, J. W. Ziller, *Angew. Chem. Int. Ed.* **2000**, *39*, 240–242; *Angew. Chem.* **2000**, *112*, 246–248; c) F. G. N. Cloke, P. B. Hitchcock, *J. Am. Chem. Soc.* **2002**, *124*, 9352–9353; d) F. G. N. Cloke, J. C. Green, N. Kaltsoyannis, *Organometallics* **2004**, *23*, 832–835; e) O. T. Summerscales, F. G. N. Cloke, P. B. Hitchcock, J. C. Green, N. Hazari, *Science* **2006**, *311*, 829–831; f) O. T. Summerscales, F. G. N. Cloke, P. B. Hitchcock, J. C. Green, N. Hazari, *J. Am. Chem. Soc.* **2006**, *128*, 9602–9603; g) A. S. Frey, F. G. N. Cloke, P. B. Hitchcock, I. J. Day, J. C. Green, G. Aitken, *J. Am. Chem. Soc.* **2008**, *130*, 13816–13817; h) F. M. Chadwick, D. M. O'Hare, *Organometallics* **2014**, *33*, 3768–3774.
- [13] a) M. Cesari, U. Pedretti, A. Zazzetta, G. Lugli, W. Marconi, *Inorg. Chim. Acta* **1971**, *5*, 439–444; b) F. A. Cotton, W. Schwotzer, *Organometallics* **1985**, *4*, 942–943.
- [14] a) S. M. Franke, B. L. Tran, F. W. Heinemann, W. Hieringer, D. J. Mendiola, K. Meyer, *Inorg. Chem.* **2013**, *52*, 10552–10558; b) H. S. La Pierre, H. Kameo, D. P. Halter, F. W. Heinemann, K. Meyer, *Angew. Chem. Int. Ed.* **2014**, *53*, 7154–7157; *Angew. Chem.* **2014**, *126*, 7282–7285; c) D. P. Halter, F. W. Heinemann, J. Bachmann, K. Meyer, *Nature* **2016**, *530*, 317–321; d) D. P. Halter, F. W. Heinemann, L. Maron, K. Meyer, *Nat. Chem.* **2018**, *10*, 259–267; e) S. C. Bart, F. W. Heinemann, C. Anthon, C. Hauser, K. Meyer, *Inorg. Chem.* **2009**, *48*, 9419–9426.
- [15] a) P. L. Arnold, J. H. Farnaby, M. G. Gardiner, J. B. Love, *Organometallics* **2015**, *34*, 2114–2117; b) B. S. Billow, B. N. Livesay, C. C. Mokhtarzadeh, J. McCracken, M. P. Shores, J. M. Boncella, A. L. Odom, *J. Am. Chem. Soc.* **2018**, *140*, 17369–17373.
- [16] T. Arliguie, M. Lance, M. Nierlich, J. Vigner, M. Ephritikhine, *J. Chem. Soc. Chem. Commun.* **1995**, *2*, 183–184.
- [17] a) N. Tsoureas, A. Mansikkamaki, R. A. Layfield, *Chem. Commun.* **2020**, *56*, 944–947; b) A. Chakraborty, B. M. Day, J. P. Durrant, M. He, J. Tang, R. A. Layfield, *Organometallics* **2020**, *39*, 8–12.
- [18] W. J. Evans, J. M. Perotti, J. C. Brady, J. W. Ziller, *J. Am. Chem. Soc.* **2003**, *125*, 5204–5212.
- [19] a) P. Scott, P. B. Hitchcock, *Polyhedron* **1994**, *13*, 1651–1653; b) P. Roussel, P. Scott, *J. Am. Chem. Soc.* **1998**, *120*, 1070–1071; c) R. Boaretto, P. Roussel, N. W. Alcock, A. J. Kingsley, I. J. Munslow, C. J. Sanders, P. Scott, *J. Organomet. Chem.* **1999**, *591*, 174–184; d) S. T. Liddle, J. McMaster, D. P. Mills, A. J. Blake, C. Jones, W. D. Woodul, *Angew. Chem. Int. Ed.* **2009**, *48*, 1077–1080; *Angew. Chem.* **2009**, *121*, 1097–1100; e) D. M. King, F. Tuna, E. J. L. McInnes, J. McMaster, W. Lewis, A. J. Blake, S. T. Liddle, *Science* **2012**, *337*, 717–720.
- [20] A. M. Tondreau, T. J. Duignan, B. W. Stein, V. E. Fleischauer, J. Autschbach, E. R. Batista, J. M. Boncella, M. G. Ferrier, S. A. Kozimor, V. Mocko, M. L. Neidig, S. K. Cary, P. Yang, *Inorg. Chem.* **2018**, *57*, 8106–8115.
- [21] A. V. Protchenko, K. H. Birj Kumar, D. Dange, A. D. Schwarz, D. Vidovic, C. Jones, N. Kaltsoyannis, P. Mountford, S. Aldridge, *J. Am. Chem. Soc.* **2012**, *134*, 6500–6503.
- [22] J. L. Kiplinger, D. E. Morris, B. L. Scott, C. J. Burns, *Organometallics* **2002**, *21*, 5978–5982.
- [23] a) H. Yin, P. J. Carroll, E. J. Schelter, *Inorg. Chem.* **2016**, *55*, 5684–5692; b) J.-C. Berthet, P. Thuery, M. Ephritikhine, *Eur. J. Inorg. Chem.* **2008**, *35*, 5455–5459; c) A. L. Odom, P. L. Arnold, C. C. Cummins, *J. Am. Chem. Soc.* **1998**, *120*, 5836–5837; d) B. Vlasisavljevich, P. L. Diaconescu, W. L. Lukens Jr., L. Gagliardi, C. C. Cummins, *Organometallics* **2013**, *32*, 1341–1352.
- [24] a) M. W. Rosenzweig, A. Scheurer, C. A. Lamsfus, F. W. Heinemann, L. Maron, J. Andrez, M. Mazzanti, K. Meyer, *Chem. Sci.* **2016**, *7*, 5857–5866; b) D. M. King, W. Lewis, S. T. Liddle, *Inorg. Chim. Acta* **2012**, *380*, 167–173; c) M. W. Rosenzweig, J. Huemmer, A. Scheurer, C. A. Lamsfus, F. W. Heinemann, L. Maron, M. Mazzanti, K. Meyer, *Dalton Trans.* **2019**, *48*, 10853–10864; d) D. R. Kindra, W. J. Evans, *Chem. Rev.* **2014**, *114*, 8865–8882; e) J. P. Day, L. M. Venanzi, *J. Chem. Soc. A* **1966**, *2*, 197–200; f) S. Fortier, J. R. Walensky, G. Wu, T. W. Hayton, *J. Am. Chem. Soc.* **2011**, *133*, 11732–11743; g) N. J. Wolford, D.-C. Sergentu, W. W. Brennessel, *J. Autschbach, M. L. Neidig, Angew. Chem. Int. Ed.* **2019**, *58*, 10266–10270; *Angew. Chem.* **2019**, *131*, 10372–10376.
- [25] a) J. P. Foster, F. Weinhold, *J. Am. Chem. Soc.* **1980**, *102*, 7211–7218; b) F. Weinhold, C. R. Landis, *Valency and Bonding: A Natural Bond Orbital Donor–Acceptor Perspective*, 1st ed., Cambridge University Press, **2005**.
- [26] D. Y. Zubarev, A. I. Boldyrev, *Phys. Chem. Chem. Phys.* **2008**, *10*, 5207–5217.
- [27] N. V. Tkachenko, A. I. Boldyrev, *Phys. Chem. Chem. Phys.* **2019**, *21*, 9590–9596.
- [28] P. Pyykko, *J. Phys. Chem. A* **2015**, *119*, 2326–2337.
- [29] R. L. Martin, *J. Chem. Phys.* **2003**, *118*, 4775–4777.

Manuscript received: January 13, 2022

Accepted manuscript online: March 14, 2022

Version of record online: April 1, 2022